1982

Broadband and narrowband signaltointerference ratio expressions for a doubly spread target

Ziomek, Lawrence J.; Sibul, Leon H.

Acoustical Society of America

The Journal of the Acoustical Society of America 72, 804 (1982); doi: 10.1121/1.388260
http://hdl.handle.net/10945/59965

Broadband and narrow-band signal-to-interference ratio expressions for a doubly spread target[a)]

Lawrence J. Ziomek
Department of Electrical Engineering, Naval Postgraduate School, Monterey, California 93940

Leon H. Sibul
Applied Research Laboratory, The Pennsylvania State University, P. O. Box 30, State College, Pennsylvania 16801

(Received 14 December 1981; accepted for publication 11 June 1982)

Signal-to-interference ratio (SIR) expressions for a doubly spread target are derived for both broadband and narrow-band transmit signals. For broadband signals, the SIR is dependent upon target and reverberation two-frequency correlation functions and upon the transmit and processing waveforms. For wide-sense stationary uncorrelated spreading (WSSUS) communication channels (which implies narrow-band transmissions), the SIR is dependent upon target and reverberation scattering functions and the cross-ambiguity function of the transmit and processing waveforms. Volume reverberation and target two-frequency correlation functions and scattering functions are *derived*. Volume reverberation is modeled as the spatially uncorrelated scattered field from randomly distributed point scatterers in deterministic plus random translational motion. A single scattering approximation is used and frequency-dependent directivity functions and attenuation due to absorption are included. A probability density function of random Doppler shift due to the random motion of the scatterers is also derived. Computer plots of the density function are presented as a function of the standard deviation of the random motion. The target is modeled as a linear array of discrete highlights in deterministic translational motion. Example scattering function calculations are presented. The volume reverberation scattering function predicts Doppler spreading as a function of both beam steering angle and random motion of the scatterers. The target scattering function also predicts a spread in Doppler values. Both scattering functions predict time spread and/or contraction as a function of Doppler spread.

PACS numbers: 43.60.Cg, 43.30.Vh

INTRODUCTION

The detection problem considered in this paper is the following binary hypothesis testing problem:

$$H_1: \tilde{r}(t) = \tilde{y}_T(t) + \tilde{y}_R(t) + \tilde{n}(t), \quad -\infty < t < \infty, \tag{1}$$

$$H_0: \tilde{r}(t) = \tilde{y}_R(t) + \tilde{n}(t), \quad -\infty < t < \infty, \tag{2}$$

where

$$\tilde{y}_T(t) = \int_{-\infty}^{\infty} \tilde{X}(f) H_T(f + f_c, t) \exp(+j2\pi f t)\, df \tag{3}$$

and

$$\tilde{y}_R(t) = \int_{-\infty}^{\infty} \tilde{X}(f) H_R(f + f_c, t) \exp(+j2\pi f t)\, df. \tag{4}$$

Hypothesis H_1 states that the complex envelope of the received signal $\tilde{r}(t)$ is equal to the sum of the complex envelopes of the target return $\tilde{y}_T(t)$, the reverberation return $\tilde{y}_R(t)$, and noise $\tilde{n}(t)$. It is assumed that $\tilde{y}_T(t)$, $\tilde{y}_R(t)$, and $\tilde{n}(t)$ are zero mean, uncorrelated random processes. It is also assumed that $\tilde{n}(t)$ is white. Hypothesis H_0 states that $\tilde{r}(t)$ is equal to the sum of the reverberation return and noise. The reverberation return, in general, is a composite of volume, surface, and bottom returns.

From Eqs. (3) and (4) it can be seen that *both* the target and reverberation (ocean medium) are being modeled as linear, time-varying, random filters. The expressions $H_T(f + f_c, t)$ and $H_R(f + f_c, t)$ are the random, time-varying, target and reverberation transfer functions, respectively. They are equal to the Fourier transforms, with respect to τ, of the *real*, time-varying, random impulse response functions $h_T(\tau, t)$ and $h_R(\tau, t)$, respectively. The expression $h(\tau, t)$ denotes the response of the filter at time t due to the application of a unit impulse at time $t - \tau$. The expression $\tilde{X}(f)$ is the Fourier transform of the input (transmit) complex envelope $\tilde{x}(t)$, and f_c is the center or carrier frequency in hertz. Equations (3) and (4) are *exact* relationships which are valid for both narrow-band and broadband transmit signals.[1]

A more common input–output relationship frequently used is

$$\tilde{y}(t) \simeq \int_{-\infty}^{\infty} \tilde{x}(t - \tau) \tilde{h}(\tau, t)\, d\tau, \tag{4a}$$

where $\tilde{h}(\tau, t)$ is the complex envelope of the real filter $h(\tau, t)$. Note, however, that Eq. (4a) is an *approximate* relationship which is based upon the assumption that both $\tilde{x}(t - \tau)$ and $\tilde{h}(\tau, t)$ are *narrow-band* signals in τ. This can be easily verified by noting that if $\tilde{h}(\tau, t)$ is in fact time invariant, i.e., if $\tilde{h}(\tau, t) = \tilde{h}(t - [t - \tau]) = \tilde{h}(\tau)$, then Eq. (4a) reduces to the familiar convolution integral

[a)] This paper is based on Chaps. 3 and 4 of L. J. Ziomek's Ph.D. dissertation "A Scattering Function Approach to Underwater Acoustic Detection and Signal Design," The Pennsylvania State University (1981).

 0001-4966/82/090804-16$00.80

$$\tilde{y}(t) \simeq \int_{-\infty}^{\infty} \tilde{x}(t-\tau)\tilde{h}(\tau)d\tau, \tag{4b}$$

which is also an approximate expression based upon a narrow-band assumption (e.g., see Van Trees[2] or Whalen[3]). Since the form of Eq. (4a) is based upon a narrow-band assumption, it is not used in this paper.

The approach of treating the ocean medium as a linear, time-varying, random communication channel is well established.[4–13] This approach has also been applied to target scattering problems in radar astronomy[14] and to communication channels in general.[15,16] However, with respect to target models, past research efforts have been devoted mainly to the slowly fluctuating point target problem.[17–24] Efforts to treat more complicated target models were made by Kooij[25] and Moose.[10] They modeled the target as a linear, *time-invariant, deterministic* filter. The target could then be considered as a singly spread target rather than as a point target. The time-invariant assumption implies no relative target motion, and hence, no target Doppler. Therefore the target return is spread in round-trip time delay values only. However, as will be demonstrated later, since the target is being modeled as a *time-varying* filter in this paper, we will obtain target return spreading in both round-trip time delay and Doppler values. Hence the designation, "doubly spread target." The concepts of a slowly fluctuating point target, a singly spread target, and a doubly spread target are discussed in Van Trees.[26] Green[14] also treated radar astronomy targets (e.g., moons and planets) as linear, time-varying, random filters.

Expressions for the signal-to-interference ratio (SIR) for a doubly spread target will be derived in Sec. I of this paper for both broadband and narrow-band transmit signals. It will be shown that in the broadband case, the SIR is dependent upon target and reverberation two-frequency correlation functions and upon the transmit and processing waveforms. For wide-sense stationary uncorrelated spreading (WSSUS) communication channels (which implies narrow-band transmissions), the SIR is dependent upon target and reverberation scattering functions and the cross-ambiguity function of the complex envelopes of the transmit and processing waveforms. In Sec. II, a *volume* reverberation two-frequency correlation function and scattering function are *derived*. In the past, assumed functional forms for the reverberation scattering function (clutter density function) were used in order to evaluate the SIR (e.g., see Refs. 10, 17, and 19). It is interesting to note that Middleton[27] (see p. 402) has stated (in the context of his reverberation model) that when the inherent random Doppler of scatterers is taken specifically into account, a scattering function cannot be defined. However, it will be demonstrated in Sec. II that for the volume reverberation model used in this paper, a volume reverberation scattering function can be defined when random motion of scatterers is included. We will restrict ourselves to volume reverberation only in this paper since derivations of surface reverberation scattering functions have appeared in the literature.[28–30] In Sec. III, a target two-frequency correlation function and scattering function are also *derived*. And finally, in Sec. IV, example calculations of volume reverberation and target scattering functions are presented.

I. THE SIGNAL-TO-INTERFERENCE RATIO FOR A DOUBLY SPREAD TARGET

A. Broadband transmit signal

The particular receiver structure used to process $\tilde{r}(t)$ is illustrated in Fig. 1. The function $\tilde{g}(t)$ is referred to as the "processing waveform." The receiver performs the following test: choose hypothesis H_1 if

$$|\tilde{l}|^2 = \left| \int_{-\infty}^{\infty} \tilde{r}(t)\tilde{g}^*(t)dt \right|^2 > \gamma \tag{5}$$

and choose H_0 otherwise. The threshold γ is chosen to satisfy a desired probability of false alarm constraint in a Neyman–Pearson test.

Let us now compute the output signal-to-interference power ratio (SIR) for the receiver shown in Fig. 1. The SIR as used in this paper is defined as

$$\text{SIR} \triangleq E\{|\tilde{l}_{\tilde{y}_T}|^2\}/E\{|\tilde{l}_{\tilde{v}}|^2\}, \tag{6}$$

where

$$\tilde{l}_{\tilde{y}_T} = \int_{-\infty}^{\infty} \tilde{y}_T(t)\tilde{g}^*(t)dt, \tag{7}$$

$$\tilde{l}_{\tilde{v}} = \int_{-\infty}^{\infty} \tilde{v}(t)\tilde{g}^*(t)dt, \tag{8}$$

and

$$\tilde{v}(t) = \tilde{y}_R(t) + \tilde{n}(t). \tag{9}$$

Using Eqs. (7)–(9), it can be shown that

$$E\{|\tilde{l}_{\tilde{y}_T}|^2\} = \int_{-\infty}^{\infty}\int_{-\infty}^{\infty} \tilde{g}^*(t)R_{\tilde{y}_T}(t,t')\tilde{g}(t')dt\,dt' \tag{10}$$

and

$$E\{|\tilde{l}_{\tilde{v}}|^2\} = \int_{-\infty}^{\infty}\int_{-\infty}^{\infty} \tilde{g}^*(t)R_{\tilde{y}_R}(t,t')\tilde{g}(t')dt\,dt' + N_0\int_{-\infty}^{\infty} |\tilde{g}(t)|^2\,dt, \tag{11}$$

where

$$R_{\tilde{y}_T}(t,t') = E\{\tilde{y}_T(t)\tilde{y}_T^*(t')\} \tag{12}$$

and

$$R_{\tilde{y}_R}(t,t') = E\{\tilde{y}_R(t)\tilde{y}_R^*(t')\}. \tag{13}$$

The parameter N_0 is the spectral height of the complex white noise $\tilde{n}(t)$, $E\{\cdot\}$ is the expectation operator, and the asterisk denotes complex conjugation.

Substituting Eqs. (10) and (11) into Eq. (6) yields

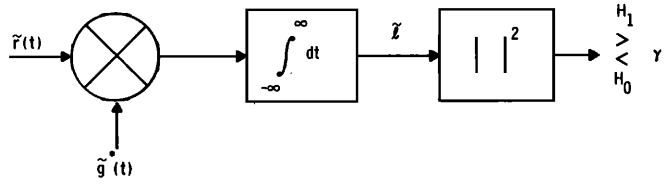

FIG. 1. Receiver structure for processing $\tilde{r}(t)$.

$$\mathrm{SIR}=\frac{\int_{-\infty}^{\infty}\int_{-\infty}^{\infty}\tilde{g}^*(t)R_{\tilde{y}_T}(t,t')\tilde{g}(t')dt\,dt'}{\int_{-\infty}^{\infty}\int_{-\infty}^{\infty}\tilde{g}^*(t)R_{\tilde{y}_R}(t,t')\tilde{g}(t')dt\,dt'+N_0\int_{-\infty}^{\infty}|\tilde{g}(t)|^2dt}, \tag{14}$$

where the autocorrelation functions of the target and reverberation returns are given by

$$R_{\tilde{y}_T}(t,t')=\int_{-\infty}^{\infty}\int_{-\infty}^{\infty}\tilde{X}(f)\tilde{X}^*(f')R_{H_T}(f+f_c,f'+f_c,t,t')\times\exp[+j2\pi(ft-f't')]df\,df' \tag{15}$$

and

$$R_{\tilde{y}_R}(t,t')=\int_{-\infty}^{\infty}\int_{-\infty}^{\infty}\tilde{X}(f)\tilde{X}^*(f')R_{H_R}(f+f_c,f'+f_c,t,t')\times\exp[+j2\pi(ft-f't')]df\,df', \tag{16}$$

where

$$R_{H_T}(f+f_c,f'+f_c,t,t')=E\{H_T(f+f_c,t)H_T^*(f'+f_c,t')\} \tag{17}$$

and

$$R_{H_R}(f+f_c,f'+f_c,t,t')=E\{H_R(f+f_c,t)H_R^*(f'+f_c,t')\}. \tag{18}$$

Equations (14) through (18) specify the SIR for a doubly spread target when either a broadband or narrow-band signal is transmitted. The autocorrelation functions given by Eqs. (17) and (18) are referred to as two-frequency correlation functions or two-frequency mutual coherence functions.[31] The significance of the two-frequency correlation function will be discussed in Sec. II. Equation (15) was obtained by substituting Eq. (3) into Eq. (12), and similarly, Eq. (16) was obtained by substituting Eq. (4) into Eq. (13).

B. Narrow-band transmit signal

If the linear, time-varying, random filters $H_T(f+f_c,t)$ and $H_R(f+f_c,t)$ are, in fact, wide-sense stationary uncorrelated spreading (WSSUS) communication channels, then the two-frequency correlation functions given by Eqs. (17) and (18) reduce to

$$R_{H_T}(f+f_c,f'+f_c,t,t')=R_{H_T}(\Delta f,\Delta t) \tag{19}$$

and

$$R_{H_R}(f+f_c,f'+f_c,t,t')=R_{H_R}(\Delta f,\Delta t), \tag{20}$$

respectively, i.e., the correlation functions are wide-sense stationary in both frequency and time[4] where $\Delta f=f-f'$ and $\Delta t=t-t'$. The expression $R_H(\Delta f,\Delta t)$ is sometimes referred to as the time-frequency correlation function.[6,9]

It will be shown in Secs. II and III that in order for the two-frequency correlation function to be wide-sense stationary in frequency, a narrow-band transmit signal must be used.[32] The condition of wide-sense stationarity in frequency does not hold for broadband transmissions.[9]

The two-frequency correlation function $R_H(\Delta f,\Delta t)$ is related to the scattering function $R_S(\tau,\phi)$ by the following two-dimensional Fourier transformations[6]:

$$R_H(\Delta f,\Delta t)=\int_{-\infty}^{\infty}\int_{-\infty}^{\infty}R_s(\tau,\phi)\exp[-j2\pi(\Delta f\tau-\phi\Delta t)]d\tau\,d\phi \tag{21}$$

and

$$R_S(\tau,\phi)=\int_{-\infty}^{\infty}\int_{-\infty}^{\infty}R_H(\Delta f,\Delta t)\times\exp[+j2\pi(\Delta f\tau-\phi\Delta t)]d\Delta f\,d\Delta t. \tag{22}$$

The scattering function can be thought of as an average power density function which determines the average amount of spread in round-trip time delay τ and frequency ϕ that a signal's power will undergo as the signal propagates through a random, time-varying, medium.[6] Note that $R_S(\tau,\phi)$ is a real, positive function of τ and ϕ.[6,9]

With the use of Eqs. (19) through (21), the autocorrelation functions of the target and reverberation returns as given by Eqs. (15) and (16), respectively, can be rewritten as

$$R_{\tilde{y}_T}(t,t')=\int_{-\infty}^{\infty}\int_{-\infty}^{\infty}\tilde{x}(t-\tau)R_{S_T}(\tau,\phi)\tilde{x}^*(t'-\tau)\times\exp(+j2\pi\phi\Delta t)d\tau\,d\phi \tag{23}$$

and

$$R_{\tilde{y}_R}(t,t')=\int_{-\infty}^{\infty}\int_{-\infty}^{\infty}\tilde{x}(t-\tau)R_{S_R}(\tau,\phi)\tilde{x}^*(t'-\tau)\times\exp(+j2\pi\phi\Delta t)d\tau\,d\phi, \tag{24}$$

where $R_{S_T}(\tau,\phi)$ and $R_{S_R}(\tau,\phi)$ are the target and reverberation scattering functions. And upon substituting Eqs. (23) and (24) into Eq. (14), one obtains

$$\mathrm{SIR}=\frac{\int_{-\infty}^{\infty}\int_{-\infty}^{\infty}R_{S_T}(\tau,\phi)|\chi_{\tilde{x}\tilde{g}}(\tau,\phi)|^2d\tau\,d\phi}{\int_{-\infty}^{\infty}\int_{-\infty}^{\infty}R_{S_R}(\tau,\phi)|\chi_{\tilde{x}\tilde{g}}(\tau,\phi)|^2d\tau\,d\phi+N_0\int_{-\infty}^{\infty}|\tilde{g}(t)|^2dt}, \tag{25}$$

where

$$\chi_{\tilde{x}\tilde{g}}(\tau,\phi)=\int_{-\infty}^{\infty}\tilde{x}\left(t-\frac{\tau}{2}\right)\tilde{g}^*\left(t+\frac{\tau}{2}\right)\exp(+j2\pi\phi t)dt \tag{26}$$

is the cross-ambiguity function of the complex envelope of the transmit signal $\tilde{x}(t)$, and the complex envelope of the processing waveform $\tilde{g}(t)$. Equation (25) is the SIR for a doubly spread target when a narrow-band signal is transmitted.

As an example, let us calculate the SIR for a slowly fluctuating point target when a narrow-band signal is transmitted. The scattering function for a slowly fluctuating point target can be expressed as[14]

$$R_{S_T}(\tau, \phi) = E\{|\tilde{b}|^2\}\delta(\tau' - \tau)\delta(\phi' - \phi), \tag{27}$$

where $E\{|\tilde{b}|^2\}$ includes the array gains, propagation losses, and scattering cross section of the target; and τ' and ϕ' are known constants. Substituting Eq. (27) into Eq. (25) yields the desired result (e.g., see DeLong and Hofstetter[18]):

$$\text{SIR} = \frac{E\{|\tilde{b}|^2\}|\chi_{\tilde{x}\tilde{g}}(\tau', \phi')|^2}{\int_{-\infty}^{\infty}\int_{-\infty}^{\infty} R_{S_R}(\tau, \phi)|\chi_{\tilde{x}\tilde{g}}(\tau, \phi)|^2 d\tau\, d\phi + N_0\int_{-\infty}^{\infty}|\tilde{g}(t)|^2\, dt}. \tag{28}$$

DeLong and Hofstetter[18] assumed that $\tau' = 0$ and $\phi' = 0$ in their expression for the SIR for a point target. If these values for τ' and ϕ' are substituted into Eq. (28), then

$$|\chi_{\tilde{x}\tilde{g}}(0, 0)|^2 = \left|\int_{-\infty}^{\infty} \tilde{x}(t)\tilde{g}^*(t)dt\right|^2, \tag{29}$$

which agrees with their result.

Note, that *no* Gaussian assumptions were made in deriving the SIR expressions given by Eqs. (14) and (25). However, when $\tilde{y}_T(t)$, $\tilde{y}_R(t)$, and $\tilde{n}(t)$ are *Gaussian*, zero mean, and uncorrelated (statistically independent) and $\tilde{n}(t)$ is white, then the error performance of the receiver shown in Fig. 1 (although it is not an optimal receiver for detecting a doubly spread target[26]) is given by

$$P_D = P_F^{1/(1+\text{SIR})}, \tag{30}$$

where P_D is the probability of detection and P_F is the probability of false alarm.[26,33] Therefore, in the important case of Gaussian statistics, maximizing the SIR is equivalent to maximizing the probability of detection for a given probability of false alarm in a Neyman–Pearson test.[21] The SIR for a doubly spread target can be maximized via signal design, i.e., by designing the transmit signal $\tilde{x}(t)$ and/or the processing waveform $\tilde{g}(t)$.[34]

One can see from Eqs. (14) and (25) that in order to evaluate or maximize the SIR for a doubly spread target for either a broadband or narrow-band transmit signal, one must be able to specify either target and reverberation two-frequency correlation functions or target and reverberation scattering functions.

II. VOLUME REVERBERATION

A. Two-frequency correlation function

Volume reverberation is the result of the scattering of energy by the inherent inhomogeneities in the ocean medium (e.g., fish, bubbles, zooplankton, etc.) and its changing index of refraction.[10,35–37] In the analysis which follows, volume reverberation is modeled as the spatially uncorrelated scattered field from randomly distributed discrete point scatterers.[38] It is assumed that the particles are undergoing translational motion. A single scattering approximation is used throughout the analysis.

We begin by considering the physical situation depicted by Fig. 2 and computing the scattered field at the receive

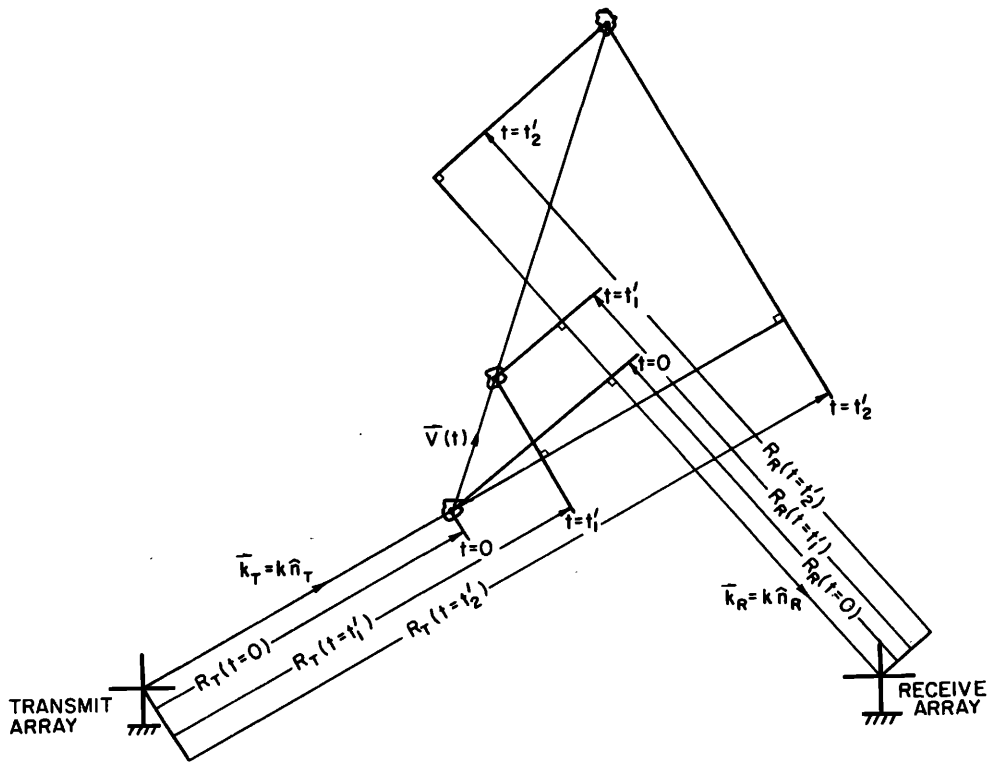

FIG. 2. Bistatic geometry for calculation of scattered field from a single particle undergoing translational motion.

array due to a single particle. Note that both the transmit and receive planar arrays are in a bistatic configuration and both are assumed not to be in motion. When transmission in the direction $\hat{n}_T$ begins at $t=0$, the range of the particle from the transmit array in the direction $\hat{n}_T$ is equal to R_{0_T}. Similarly, the range of the particle from the receive array in the direction $-\hat{n}_R$ at $t=0$ is equal to R_{0_R}. Both $\hat{n}_T$ and $\hat{n}_R$ are unit vectors. The particle's motion is described by the time-varying translational velocity vector $\mathbf{V}(t)$. Therefore the range of the particle from the transmit array at any time t, in the direction $\hat{n}_T$, is given by

$$R_T(t) = R_{0_T} + \int_0^t \mathbf{V}(t)\cdot\hat{n}_T\, dt \tag{31}$$

and similarly, the range of the particle from the receive array at any time t, in the direction $-\hat{n}_R$, is

$$R_R(t) = R_{0_R} + \int_0^t \mathbf{V}(t)\cdot(-\hat{n}_R)dt. \tag{32}$$

Assume that a unit amplitude, time-harmonic signal is transmitted and that the moving particle is in the farfield region of both the transmit and receive arrays. At some time instant, say $t=t_1'$, the time-harmonic signal transmitted in the direction $\hat{n}_T$ is incident upon the particle and some power is scattered towards the receive array in the direction $\hat{n}_R$. The scattered acoustic pressure field begins to appear at the output of the receive array at time t_1, where

$$t_1 = t_1' + R_R(t_1')/c, \tag{33}$$

t_1' is the retarded time, and c is the speed of sound (in m/s) in the medium and is assumed to be constant. The output at time t_1 is given by

$$y(t_1) = \mathrm{Re}[H(f,t_1)\exp(+j2\pi f t_1)], \tag{34}$$

where

$$H(f,t_1) = D_T(k_{x_T},k_{y_T})g(\hat{n}_R,\hat{n}_T,f)D_R(k_{x_R},k_{y_R}) \times \frac{\exp[-jkR_T(t_1')]}{R_T(t_1')}\exp[-\alpha_T(f)R_T(t_1')] \times \frac{\exp[-jkR_R(t_1')]}{R_R(t_1')}\exp[-\alpha_R(f)R_R(t_1')] \tag{35}$$

when the transmit signal $x(t)=\mathrm{Re}[\exp(+j2\pi f t)]$.

Equation (35) is the random, time-varying, transfer function of the communication channel corresponding to the physical situation of a single particle in translational motion with respect to a bistatic transmit/receive array geometry. The expressions D_T and D_R are the farfield directivity patterns of the transmit and receive arrays, respectively. The farfield directivity pattern of an acoustic planar array is given by the two-dimensional Fourier transform of the spatial distribution of normal driving velocity, say $v(x,y)$; i.e.,

$$D(k_x,k_y) = \iint_R v(x,y)\exp[+j(k_x x + k_y y)]\,dx\,dy \tag{36}$$

when the baffle surrounding the active region R is assumed to be rigid.[39] The x and y components of the wavenumber k are given by

$$k_x = k\sin\theta\cos\psi = ku \tag{37}$$

and

$$k_y = k\sin\theta\sin\psi = kv, \tag{38}$$

where

$$k = 2\pi f/c = 2\pi/\lambda. \tag{39}$$

The terms $u=\sin\theta\cos\psi$ and $v=\sin\theta\sin\psi$ are the direction cosines with respect to the positive X and Y axes, respectively. The expressions α_T and α_R are the frequency dependent amplitude attenuation coefficients due to sound absorption, with units of nepers/meters, along the transmit and receive paths, respectively.

The function $g(\hat{n}_R,\hat{n}_T,f)$ is referred to as the scattering amplitude function.[40] It represents the random farfield amplitude of the scattered wave in the direction $\hat{n}_R$ when the particle is illuminated (insonified) by a unit amplitude plane wave propagating in the direction $\hat{n}_T$.

In order to simplify Eq. (35), assume that the velocity of the particle is constant during the time it is insonified, i.e., $\mathbf{V}(t)=\mathbf{V}$ and that

$$R_{0_T} \gg \int_0^{t_1'} \mathbf{V}(t)\cdot\hat{n}_T\, dt \tag{40}$$

and

$$R_{0_R} \gg \int_0^{t_1'} \mathbf{V}(t)\cdot(-\hat{n}_R)dt. \tag{41}$$

Also assume that $\alpha_T(f)=\alpha_R(f)=\alpha(f)$. Therefore, upon using these assumptions [Eqs. (40) and (41) are only used in simplifying the denominator], Eq. (35) reduces to

$$H(f,t_1) = F(f)\frac{\exp\{-jk_{\mathrm{eff}}[R_{0_T}+R_{0_R}+(\hat{n}_T-\hat{n}_R)\cdot\mathbf{V}t_1']\}}{R_{0_T}R_{0_R}}, \tag{42}$$

where

$$t_1' = (t_1 - R_{0_R}/c)/(1-\mathbf{V}\cdot\hat{n}_R/c), \tag{43}$$

$$F(f) \triangleq D_T(k_{x_T},k_{y_T})g(\hat{n}_R,\hat{n}_T,f)D_R(k_{x_R},k_{y_R}) \tag{44}$$

and k_{eff} is the complex effective wavenumber defined by

$$k_{\mathrm{eff}} \triangleq k - j\alpha(f). \tag{45}$$

Since the transfer function given by Eq. (42) is random, it is more appropriate to characterize the scattered field by the two-frequency correlation function. If we consider a unit volume element dV and assume that the particles occupying dV are characterized by identical parameters (e.g., scattering amplitude functions and translational velocity vectors) and that the fields scattered from these particles are uncorrelated, then the volume reverberation two-frequency correlation function corresponding to dV is given by

$$R_{H_R}(f+f_c, f'+f_c, t, t') = R_H(f+f_c, f'+f_c, t, t')\rho_V\, dV, \quad (46)$$

where ρ_V is the volume density function of the point scatterers (number of scatterers per unit volume) and $R_H(f+f_c, f'+f_c, t, t')$ is the correlation function of Eq. (42). With the use of Eqs. (42) through (45) and upon integrating the right-hand side of Eq. (46) over the scattering volume V, which is common to both the transmit and receive arrays, it can be shown that the following general bistatic expression for the volume reverberation two-frequency correlation function is obtained:

$$\begin{aligned} R_{H_R}(f+f_c, f'+f_c, t_1, t_2) &= \int_V E\{F(f+f_c)F^*(f'+f_c)\} E\left\{\exp\left[-j2\pi\left[\left(1+\frac{f}{f_c}\right)t_1 - \left(1+\frac{f'}{f_c}\right)t_2\right]\phi\right]\right. \\ &\times \exp[+j2\pi(f-f')(\phi/f_c)(R_{0_R}/c)]\exp\{-[\alpha(f+f_c)(t_1 - R_{0_R}/c) + \alpha(f'+f_c)(t_2 - R_{0_R}/c)][(\hat{n}_T - \hat{n}_R)\cdot\mathbf{V}]\}\Big] \\ &\times \exp\{-[\alpha(f+f_c)+\alpha(f'+f_c)](R_{0_T}+R_{0_R})\}\exp\{-j2\pi[(R_{0_T}+R_{0_R})/c](f-f')\}(\rho_V/R_{0_T}^2 R_{0_R}^2)dV, \end{aligned} \quad (47)$$

where, from Eq. (44),

$$\begin{aligned} E\{F(f+f_c)F^*(f'+f_c)\} &= D_T(k_1u_T, k_1v_T)D_T^*(k_2u_T, k_2v_T) \\ &\times E\{g(\hat{n}_R, \hat{n}_T, f_1)g^*(\hat{n}_R, \hat{n}_T, f_2)\}D_R(k_1u_R, k_1v_R)D_R^*(k_2u_R, k_2v_R), \end{aligned} \quad (48)$$

where

$$k_i = 2\pi f_i/c; \quad i = 1, 2, \quad (49)$$

$$f_1 = f + f_c, \quad (50)$$

and

$$f_2 = f' + f_c; \quad (51)$$

and

$$\phi \triangleq f_c(\hat{n}_T - \hat{n}_R)\cdot\mathbf{V}/c \quad (52)$$

is the bistatic Doppler shift where it has been assumed that $|\mathbf{V}|/c \ll 1$. In general, $\mathbf{V}$ can be expressed as the sum of a deterministic component $\mathbf{U}$, and a random or fluctuating component $\mathbf{V}_f$.

The derivation of Eq. (47) was based upon the assumption that the scattered fields from different spatial locations within V are *uncorrelated*. For simplicity, all particles within the common scattering volume V are assumed to be characterized by the same scattering amplitude function $g(\hat{n}_R, \hat{n}_T, f)$ and velocity vector $\mathbf{V}$. Otherwise, $g(\hat{n}_R, \hat{n}_T, f)$ and $\mathbf{V}$ have to be shown as functions of position within V. Note, however, $g(\hat{n}_R, \hat{n}_T, f)$ is still a function of geometry because of its dependence upon $\hat{n}_T$ and $\hat{n}_R$.

For a monostatic transmit/receive array geometry, let

$$R_{0_T} = R_{0_R} = r, \quad u_T = u_R = u, \quad v_T = v_R = v, \quad (53)$$

and

$$\hat{n}_R = -\hat{n}_T.$$

Ishimaru[31] refers to the autocorrelation function of the random, time-varying transfer function $R_H(f, f', t, t') = E\{H(f,t)H^*(f',t')\}$ as the two-frequency correlation function or the two-frequency mutual coherence function. The expression $R_H(f,f',t,t')$ is equal to the amount of correlation which exists between the output fields $H(f, t)$ and $H(f', t')$ at two different times (t and t') due to the application of time-harmonic input fields at two different frequencies (f and f'). If two time-harmonic waves are transmitted at the same frequency f, and the resulting output fields are observed at two different times t and t', the correlation between the output fields *decreases* as the time difference $\Delta t = t - t'$ *increases*.[31] The value of the time difference Δt at which the correlation function $R_H(f,f,t,t') = E\{H(f,t)H^*(f,t')\}$ is approximately equal to zero or decreases to a specified level is called the *coherence time*.[31] The reciprocal of the coherence time is equal to the amount of frequency spread a wave will undergo as it propagates in a random, time-varying medium.[31]

Similarly, if two time-harmonic waves are transmitted at two different frequencies f and f', and the resulting output fields are observed at the same time t, the correlation between the two output fields *decreases* as the frequency difference $\Delta f = f - f'$ *increases*.[31] The value of the frequency difference Δf at which the correlation function $R_H(f,f',t,t) = E\{H(f,t)H^*(f',t)\}$ is approximately equal to zero or decreases to a specified level is called the *coherence bandwidth*.[31] The reciprocal of the coherence bandwidth is equal to the amount of spread in round-trip time delay a wave will undergo as it propagates in a random, time-varying medium.[31]

Therefore both the coherence time and the coherence bandwidth, and hence, the frequency and time delay spreading associated with our model of volume reverberation, can be computed from Eq. (47). With the use of Eq. (47), the autocorrelation function $R_{\bar{y}_R}(t, t')$, which is given by Eq. (16) and appears in the SIR expression given by Eq. (14), can now be computed.

B. Scattering function

Since R_{H_R} as given by Eq. (47) is not a function of Δf and Δt, the volume reverberation scattering function cannot

be obtained from it via the two-dimensional Fourier transformation given by Eq. (22). However, if it is assumed that the transmit signal is *narrow band*, it can be shown that Eq. (47) reduces to a function of Δf and Δt. Therefore let us assume that the transmit signal is indeed narrow band, and as a result, it is reasonable to assume that $|f| \ll f_c$ and $|f'| \ll f_c$ so that[32]

$$E\{F(f+f_c)F^*(f'+f_c)\} \simeq E\{|F(f_c)|^2\}, \tag{54}$$

$$\alpha(f+f_c) \simeq \alpha(f_c), \tag{55}$$

and

$$\alpha(f'+f_c) \simeq \alpha(f_c). \tag{56}$$

Note that the term narrow band is used to describe a transmit signal vis-à-vis broadband whenever the approximations given by Eqs. (54) through (56) are valid.[5,32]

Using Eqs. (54) through (56) and the assumptions that $|f|/f_c \ll 1$ and $|f'|/f_c \ll 1$, Eq. (47) can now be written as

$$R_{H_R}(\Delta f, t_1, t_2) = \int_V E\{|F(f_c)|^2\} E\left\{\exp(-j2\pi\phi\Delta t)\exp\left[+j2\pi\Delta f\left(\frac{\phi}{f_c}\right)\left(\frac{R_{0_R}}{c}\right)\right]\exp\{-\alpha(f_c)[(t_1+t_2)-2R_{0_R}/c]\right.$$
$$\left.\times[(\hat{n}_T-\hat{n}_R)\cdot\mathbf{V}]\}\right\}\exp[-2\alpha(f_c)(R_{0_T}+R_{0_R})]\exp\{-j2\pi[(R_{0_T}+R_{0_R})/c]\Delta f\}(\rho_V/R_{0_T}^2 R_{0_R}^2)dV, \tag{57}$$

where $\Delta f = f - f'$ and $\Delta t = t_1 - t_2$. The two-frequency correlation function is still *not* a function of Δt due to the presence of the term $t_1 + t_2$ appearing in the third exponential factor, involving attenuation due to sound absorption.

Now, with regard to the significance of the third exponential factor appearing in the integrand of Eq. (57) to attenuation, consider the following order of magnitude argument. The time instants t_1 and t_2 correspond to the times at which reverberation returns are monitored at the receive array and are approximately equal to

$$t_1 \simeq (R_{0_T} + R_{0_R})/c \tag{58}$$

and

$$t_2 \simeq (R_{0_T} + R_{0_R})/c + \delta t, \tag{59}$$

where δt is some relatively small time increment since it is assumed that $t_2 > t_1$. Therefore, using Eqs. (58) and (59), it can be shown that

$$\exp\{-\alpha(f_c)[(t_1+t_2)-2R_{0_R}/c][(\hat{n}_T-\hat{n}_R)\cdot\mathbf{V}]\}$$
$$\simeq \exp\{-\alpha(f_c)(2R_{0_T}+c\delta t)[(\hat{n}_T-\hat{n}_R)\cdot\mathbf{V}/c]\}, \tag{60}$$

which is negligible compared to the attenuation due to

$$\exp[-\alpha(f_c)(2R_{0_T}+2R_{0_R})]$$

and can therefore be ignored. Making use of this observation and assuming that $\mathbf{V}$ can be expressed as the sum of a deterministic and random component, Eq. (57) finally reduces to the desired result:

$$R_{H_R}(\Delta f, \Delta t) = \int_V E\{|F(f_c)|^2\}\exp\left\{-j2\pi\left[\Delta t - \left(\frac{\Delta f}{f_c}\right)\left(\frac{R_{0_R}}{c}\right)\right]\phi_{\text{det}}\right\}$$
$$\times E\{\exp\{-j2\pi[\Delta t - (\Delta f/f_c)(R_{0_R}/c)]\phi_{\text{RND}}\}\}\exp[-2\alpha(f_c)(R_{0_T}+R_{0_R})]$$
$$\times\exp\{-j2\pi[(R_{0_T}+R_{0_R})/c]\Delta f\}(\rho_V/R_{0_T}^2 R_{0_R}^2)dV, \tag{61}$$

where ϕ_{det} is the deterministic, bistatic Doppler shift defined as

$$\phi_{\text{det}} \triangleq [f_c(\hat{n}_T - \hat{n}_R)\cdot\mathbf{U}]/c, \tag{62}$$

$\mathbf{U}$ being the deterministic component of the velocity vector $\mathbf{V}$; and ϕ_{rnd} is the random, bistatic Doppler shift defined as

$$\phi_{\text{rnd}} \triangleq [f_c(\hat{n}_T - \hat{n}_R)\cdot\mathbf{V}_f]/c, \tag{63}$$

$\mathbf{V}_f$ being the fluctuating or random component of $\mathbf{V}$. Note that the Doppler shifts ϕ_{det} and ϕ_{rnd} are functions of angle due to the presence of the inner product. For example, in the spherical coordinate system, ϕ_{det} is a function of the spherical angles (θ, ψ). And since the directivity patterns D_T and D_R are also functions of (θ, ψ), different deterministic Doppler shifts are weighted differently by the beam patterns. Thus a Doppler spread will result because of the finite extent of the beamwidths of both the transmit and receive beam patterns.

Now upon substituting Eq. (61) into Eq. (22) and integrating, one obtains the following bistatic expression for the volume reverberation scattering function:

$$R_{S_R}(\tau, \phi) = \int_V E\{|F(f_c)|^2\}\, p_{\phi_{\text{rnd}}}(\phi + \phi_{\text{det}})\delta[\tau - \tau(\phi)]$$
$$\times\exp[-2\alpha(f_c)(R_{0_T}+R_{0_R})]$$
$$\times(\rho_V/R_{0_T}^2 R_{0_R}^2)dV, \tag{64}$$

which is a function of the time delay τ (in seconds) and the Doppler spread ϕ (in hertz), where

$$\tau(\phi) \triangleq \tau_0 + [(\phi R_{0_R})/(f_c c)], \tag{65}$$

$$\tau_0 \triangleq (R_{0_T} + R_{0_R})/c, \tag{66}$$

and

$$E\{|F(f_c)|^2\} = |D_T(ku_T, kv_T)|^2 E\{|g(\hat{n}_R, \hat{n}_T, f_c)|^2\}$$
$$\times|D_R(ku_R, kv_R)|^2, \tag{67}$$

where $k = 2\pi f_c/c$ and $p_{\phi_{\text{rnd}}}(\cdot)$ is the probability density function of the random Doppler shift given by

$$p_{\phi_{\rm rnd}}(\phi) = \left(\frac{c}{|\hat{n}_T - \hat{n}_R| f_c \sigma}\right)^3 \frac{\sqrt{2}}{\pi\sqrt{\pi}} \int_{|\phi|}^{\infty} \frac{x^2}{(x^2 - \phi^2)^{1/2}} \times \exp\left[-\frac{1}{2}\left(\frac{c}{|\hat{n}_T - \hat{n}_R| f_c \sigma}\right)^2 x^2 \right] dx; \quad |\phi| < x < \infty, \tag{68}$$

where σ is the standard deviation of $|\mathbf{V}_f|$. Middleton[27] (see p. 402) has stated (in the context of his reverberation model) that when the inherent random Doppler of scatterers is taken specifically into account, a scattering function cannot be defined. However, the volume reverberation scattering function given by Eq. (64) demonstrates that for the volume reverberation model used in this paper, a scattering function can be defined when random motion of scatterers is included.

Note that $\tau(\phi)$ as defined by Eq. (65) is *not* the round-trip time delay. However, it is shown in Ziomek[41,42] that the round-trip time delay can be obtained from $\tau(\phi)$ by dividing it by the dimensionless scale factor $[1 + (\phi/f_c)]$. That is, the round-trip time delay is a function of the Doppler spread ϕ (which agrees with Middleton's[5] observations) and is given by $\tau(\phi)/[1 + (\phi/f_c)]$. This will be demonstrated in Sec. IVB when a target scattering function is computed. An in-depth discussion of Doppler effects can be found in Middleton.[43]

The derivation of the probability density function of the random variable

$$\phi_{\rm rnd} \triangleq f_c(\hat{n}_T - \hat{n}_R)\cdot\mathbf{V}_f/c = f_c|\hat{n}_T - \hat{n}_R|\,|\mathbf{V}_f|\cos\xi/c \tag{69}$$

can be found in the Appendix and was based upon the assumptions that $|\mathbf{V}_f|$ was Maxwell distributed, the angle ξ was uniformly distributed, and that the random variables $|\mathbf{V}_f|$ and $\cos\xi$ are statistically independent. Figures 3 and 4 are plots of the probability density function given by Eq. (68) for a monostatic geometry ($\hat{n}_R = -\hat{n}_T$) for $\sigma = 0.1$ m/s and $\sigma = 1.0$ m/s, respectively. As one might expect, when the random motion increases (increasing σ), the Doppler spread increases.

The function $E\{|g(\hat{n}_R, \hat{n}_T, f_c)|^2\} \equiv \sigma_d(\hat{n}_R, \hat{n}_T, f_c)$ and is

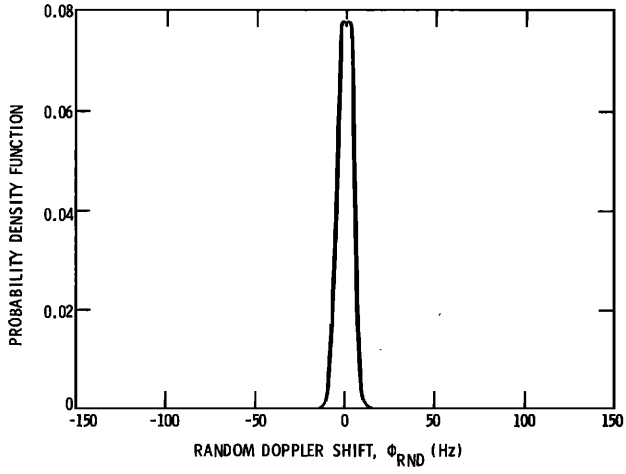

FIG. 3. Probability density function of the random Doppler shift for a monostatic transmit/receive array geometry ($\sigma = 0.1$ m/s).

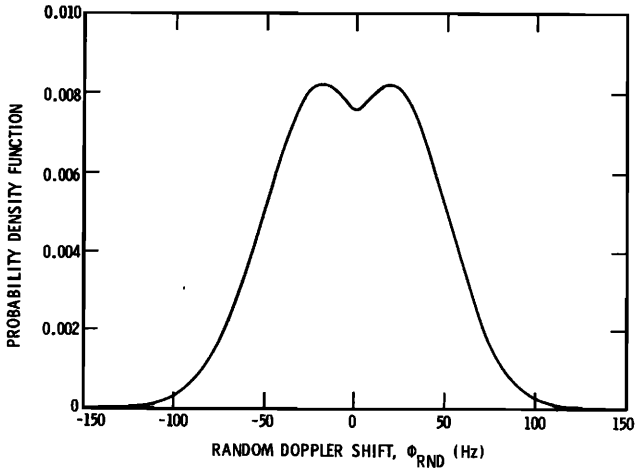

FIG. 4. Probability density function of the random Doppler shift for a monostatic transmit/receive array geometry ($\sigma = 1.0$ m/s).

referred to as the average differential scattering cross section of one of the point scatterers and has units of area.[40,44,45] The average bistatic radar cross section is equal to

$$4\pi E\{|g(\hat{n}_R, \hat{n}_T, f_c)|^2\} = 4\pi\sigma_d(\hat{n}_R, \hat{n}_T, f_c).$$

In the case of a monostatic geometry, the average backscatter radar cross section of one of the point scatterers is equal to

$$4\pi E\{|g(-\hat{n}_T, \hat{n}_T, f_c)|^2\} = 4\pi\sigma_d(-\hat{n}_T, \hat{n}_T, f_c).$$

The *target strength* of an individual point scatter is given by[45]

$$10\log_{10}[\sigma_d(-\hat{n}_T, \hat{n}_T, f_c)/A_1]\,\text{dB } re: A_1, \tag{70}$$

where $A_1 = 1$ m^2 and *re* means "relative to." Thus the target strength or *volume reverberation backscattering strength* is a decibel measure of the differential backscattering cross section.[44,45] The volume reverberation backscattering strength is dependent upon the type and density of scatterers per unit volume.[44,45] For example, the backscattering strength per unit volume is given by[45]

$$10\log_{10}[\rho_V\sigma_d(-\hat{n}_T, \hat{n}_T, f_c)R_1]\,\text{dB } re: R_1, \tag{71}$$

where ρ_V is the volume density of the scatterers and R_1 is the reference distance, ususally chosen to be 1 m.

As an example, the average received energy (in dB) from volume reverberation will be computed from the expression[46]

$$\overline{E}_y = E_x \int_{-\infty}^{\infty}\int_{-\infty}^{\infty} R_{S_R}(\tau, \phi)\,d\tau\,d\phi, \tag{72}$$

where $\overline{E}_y$ is the average received energy, E_x is the transmit energy, and $R_{S_R}(\tau, \phi)$ is the volume reverberation scattering function given by Eq. (64). For simplicity, assume a monostatic transmit/receive array geometry [see Eq. (53)] and no motion, i.e., $\phi_{\rm det} = \phi_{\rm rnd} = 0$; and as a result, $p_{\phi_{\rm rnd}}(\phi + \phi_{\rm det}) = p_{\phi_{\rm rnd}}(\phi) \equiv \delta(\phi)$. With these assumptions, Eq. (64) reduces to

$$R_{S_R}(\tau, \phi) = \int_V E\{|F(f_c)|^2\}\delta(\phi)\delta\left[\tau - \left(\frac{2r}{c} + \frac{\phi}{f_c}\frac{r}{c}\right)\right] \times \exp[-4\alpha(f_c)r](\rho_V/r^4)dV \tag{73}$$

or

$$R_{S_R}(\tau, \phi) = R_{S_R}(\tau)\delta(\phi), \tag{74}$$

where

$$R_{S_R}(\tau) = \int_V E\{|F(f_c)|^2\}\delta\left(\tau - \frac{2r}{c}\right) \times \exp[-4\alpha(f_c)r](\rho_V/r^4)dV \tag{75}$$

and from Eqs. (53) and (67),

$$E\{|F(f_c)|^2\} = |D_T(ku, kv)|^2\sigma_d(-\hat{n}_T, \hat{n}_T, f_c) \times |D_R(ku, kv)|^2. \tag{76}$$

Now, if Eq. (74) is substituted into Eq. (72), one obtains

$$\overline{E}_y = E_x\int_{-\infty}^{\infty} R_{S_R}(\tau)d\tau \tag{77}$$

and substituting Eq. (75) into Eq. (77) yields

$$\overline{E}_y = E_x\int_V E\{|F(f_c)|^2\}\left[\int_{-\infty}^{\infty}\delta\left(\tau - \frac{2r}{c}\right)d\tau\right] \times \exp[-4\alpha(f_c)r](\rho_V/r^4)dV \tag{78}$$

or

$$\overline{E}_y = E_x\int_V E\{|F(f_c)|^2\}\exp[-4\alpha(f_c)r]\left(\frac{\rho_V}{r^4}\right)dV. \tag{79}$$

Next, assume a spherical coordinate system so that $dV = r^2 \sin\theta\, dr\, d\theta\, d\psi$, and that ρ_V is not a function of position. In addition, assume that $\sigma_d(-\hat{n}_T, \hat{n}_T, f_c)$ does not depend upon $\hat{n}_T$, i.e., assume that $\sigma_d(-\hat{n}_T, \hat{n}_T, f_c)$ is omnidirectional and is equal to a constant σ_d. Therefore, with these assumptions, Eq. (79) can be expressed as

$$\overline{E}_y = E_x(\rho_V\sigma_d)\int_{r-(\Delta r/2)}^{r+(\Delta r/2)}\frac{\exp[-4\alpha(f_c)r]}{r^4}r^2\,dr \times\int_{\theta=0}^{\pi/2}\int_{\psi=0}^{2\pi}|D_T(ku, kv)|^2|D_R(ku, kv)|^2\sin\theta\,d\theta\,d\psi, \tag{80}$$

where $k = 2\pi f_c/c$, $u = \sin\theta\cos\psi$ and $v = \sin\theta\sin\psi$. If it is further assumed that the range interval Δr is negligible compared to r, then the integrand of the range integral is approximately constant so that

$$\int_{r-(\Delta r/2)}^{r+(\Delta r/2)}\frac{\exp[-4\alpha(f_c)r]}{r^4}r^2\,dr \simeq\{\exp[-4\alpha(f_c)r]r^{-4}\}(r^2\Delta r) \tag{81}$$

and as a result, Eq. (80) finally simplifies to

$$\overline{E}_y = E_x(\rho_V\sigma_d)\{\exp[-4\alpha(f_c)r]r^{-4}\}(r^2\Delta r\Psi), \tag{82}$$

where

$$\Psi = \int_{\theta=0}^{\pi/2}\int_{\psi=0}^{2\pi}|D_T(ku, kv)|^2|D_R(ku, kv)|^2\sin\theta\,d\theta\,d\psi. \tag{83}$$

Therefore the average received energy from volume reverberation in decibels is

$$10\log_{10}\overline{E}_y = 10\log_{10}E_x + 10\log_{10}(\rho_V\sigma_d) - 40\log_{10}r + 10\log_{10}\{\exp[-4\alpha(f_c)r]\} + 10\log_{10}(r^2\Delta r\Psi). \tag{84}$$

Equation (84) is the sonar equation for volume reverberation level (e.g., see Urick[44]) since (1) $10\log_{10}E_x$ is the source level, (2) $10\log_{10}(\rho_V\sigma_d)$ is the volume reverberation backscattering strength per unit volume, (3) $-40\log_{10}r$ is the two-way transmission loss due to spherical spreading, (4) $10\log_{10}\{\exp[-4\alpha(f_c)r]\}$ is the two-way transmission loss due to sound absorption, and (5) the expression $r^2\Delta r\Psi$ corresponds to what Urick[44] calls the "reverberating volume."

And finally, for the sole purpose of comparison, an alternate expression for the volume reverberation scattering function, as is found in Moose,[10] will be presented. As Moose[10] indicates, several researchers (e.g., see Refs. 5, 35, and 47) have modeled the reverberation return as

$$\tilde{y}_R(t) = \sum_{i=1}^{N(t)} a_i\tilde{x}(t - \tau_i)\exp(+j2\pi\phi_i t), \tag{85}$$

where $N(t)$ is a Poisson random variable which governs the number of reflections from the discrete point scatterers that contribute to the sum at time t. The a_i are random coefficients which include all such factors as transducer patterns, propagation loss, and the cross sections of the scatterers. If the a_i are zero mean, statistically independent random variables, then Moose[10] shows that the autocorrelation function $R_{\tilde{y}_R}(t, t')$ of Eq. (85) is of the same form as Eq. (24) and that the scattering function is given by

$$R_{S_R}(\tau, \phi) = E\{|a(\tau, \phi)|^2\}\rho(\tau, \phi), \tag{86}$$

where $E\{|a(\tau, \phi)|^2\} \sim E\{|a_i|^2\}$ for scatterers with ranges and Doppler shifts near (τ, ϕ), and $\rho(\tau, \phi)$ is the Poisson parameter which describes the density of scatterers near (τ, ϕ), i.e.,

$$P(N; \tau, \phi) = \frac{[\rho(\tau, \phi)\Delta\tau\Delta\phi]^N}{N!}\exp\{-[\rho(\tau, \phi)\Delta\tau\Delta\phi]\} \tag{87}$$

is the probability that exactly N scatterers have Doppler shifts between ϕ and $\phi + \Delta\phi$ and time delays between τ and $\tau + \Delta\tau$. The product $\rho(\tau, \phi)\Delta\tau\Delta\phi$ is the expected number of scatterers in the area $\Delta\tau\Delta\phi$.

The differences between the volume reverberation scattering functions given by Eqs. (64) and (86) are obvious.

The scattering function given by Eq. (64) can be substituted into the SIR expression of Eq. (25).

III. TARGET

A. Two-frequency correlation function

The target is modeled as a linear array of discrete highlights in deterministic translational motion. Each highlight is characterized by its own average differential scattering cross section. The scattered acoustic pressure fields from the individual highlights are assumed to be uncorrelated. Only a monostatic array geometry will be considered.

In order to derive a monostatic expression for the two-frequency correlation function for a simple line target composed of discrete point scatterers, start with the following monostatic form of the volume reverberation two-frequency correlation function in the spherical coordinate system obtained from Eq. (47):

$$R_{H_T}(f+f_c,f'+f_c,t_1,t_2) = \int_r\int_\theta\int_\psi E\{F(f+f_c)F^*(f'+f_c)\}\exp\left\{-j2\pi\left[\left(1+\frac{f}{f_c}\right)t_1-\left(1+\frac{f'}{f_c}\right)t_2\right]\phi_{\text{det}}\right\}$$
$$\times\exp\left[+j2\pi(f-f')\left(\frac{\phi_{\text{det}}}{f_c}\right)\left(\frac{r}{c}\right)\right]\exp\left\{-\left[\alpha(f+f_c)\left(t_1-\frac{r}{c}\right)+\alpha(f'+f_c)\left(t_2-\frac{r}{c}\right)\right](2\hat{n}_T\cdot\mathbf{U})\right\}$$
$$\times\exp\{-2r[\alpha(f+f_c)+\alpha(f'+f_c)]\}\exp[-j2\pi(2r/c)(f-f')]\,\rho_V(1/r^2)\sin\theta\,dr\,d\theta\,d\psi, \tag{88}$$

where

$$\phi_{\text{det}} = 2f_c\hat{n}_T\cdot\mathbf{U}/c \tag{89}$$

is the deterministic, monostatic Doppler shift since the velocity vector **V** in Eqs. (47) and (52) was set equal to **U** since it was assumed that the target, and hence, the scatterers, have only deterministic translational motion. The problem now is to mathematically represent the volume density function ρ_V of the scatterers.

Toward this end, refer to Fig. 5 where the line target is represented by the vector $\mathbf{r}_{AB}$. The length of the target is $|\mathbf{r}_{AB}| = L$ m and it has a velocity vector $\mathbf{U} = |\mathbf{U}|\hat{n}_{AB}$, where $\hat{n}_{AB}$ is a unit vector in the direction of $\mathbf{r}_{AB}$. Thus all the highlights will have the same velocity vector **U**. Both the transmit and receive arrays lie in the XY plane. The relative orientation of the target with respect to the arrays is specified by the position vectors $\mathbf{r}_A$ and $\mathbf{r}_B$ to the endpoints A and B of the target, respectively. Note that $\mathbf{r}_{AB} = \mathbf{r}_B - \mathbf{r}_A$. The vector $\mathbf{r} = \mathbf{r}_A + d\hat{n}_{AB}$ is the position vector to any discrete highlight along the target. Any particular highlight is designated by its distance d (in meters) from endpoint A.

Therefore the volume density function can be expressed as

$$\rho_V(r,\theta,\psi) = \sum_{n=1}^{N}\delta(r-r_n)\delta(\theta-\theta_n)\delta(\psi-\psi_n), \tag{90}$$

where the spherical coordinates (r_n, θ_n, ψ_n) of the nth highlight are given by

$$r_n = |\mathbf{r}_n| = \left\{\left[\left(1-\frac{d_n}{L}\right)|\mathbf{r}_A|u_A+\frac{d_n}{L}|\mathbf{r}_B|u_B\right]^2 + \left[\left(1-\frac{d_n}{L}\right)|\mathbf{r}_A|v_A+\frac{d_n}{L}|\mathbf{r}_B|v_B\right]^2 + \left[\left(1-\frac{d_n}{L}\right)|\mathbf{r}_A|w_A+\frac{d_n}{L}|\mathbf{r}_B|w_B\right]^2\right\}^{1/2}, \tag{91}$$

$$\theta_n = \cos^{-1}\left\{\frac{1}{r_n}\left[\left(1-\frac{d_n}{L}\right)|\mathbf{r}_A|w_A+\frac{d_n}{L}|\mathbf{r}_B|w_B\right]\right\}, \tag{92}$$

and

$$\psi_n = \cos^{-1}\left\{\frac{1}{r_n\sin\theta_n}\left[\left(1-\frac{d_n}{L}\right)|\mathbf{r}_A|u_A+\frac{d_n}{L}|\mathbf{r}_B|u_B\right]\right\}, \tag{93}$$

where

$$\begin{aligned} u_A &= \sin\theta_A\cos\psi_A, & u_B &= \sin\theta_B\cos\psi_B,\\ v_A &= \sin\theta_A\sin\psi_A, & v_B &= \sin\theta_B\sin\psi_B,\\ w_A &= \cos\theta_A, & w_B &= \cos\theta_B, \end{aligned} \tag{94}$$

where u_A and u_B, v_A and v_B, and w_A and w_B are the direction cosines of endpoints A and B of the line target with respect to the positive X, Y, and Z axes, respectively; and N is the total number of highlights. The parameter d_n is the distance (in meters) of the nth highlight from endpoint A. Equations (91)–(94) describe the monostatic geometry at the time instant when *transmission begins* (i.e., at $t = 0$).

Substituting Eq. (90) into Eq. (88) yields the following monostatic expression for the target two-frequency correlation function:

$$R_{H_T}(f+f_c,f'+f_c,t_1,t_2)$$
$$= \sum_{n=1}^{N} E\{F_n(f+f_c)F_n^*(f'+f_c)\}\exp\left\{-j2\pi\left[\left(1+\frac{f}{f_c}\right)t_1-\left(1+\frac{f'}{f_c}\right)t_2\right]\phi_{\text{det}_n}\right\}$$
$$\times\exp\left[+j2\pi(f-f')\left(\frac{\phi_{\text{det}_n}}{f_c}\right)\left(\frac{r_n}{c}\right)\right]\exp\left\{-\left[\alpha(f+f_c)\left(t_1-\frac{r_n}{c}\right)+\alpha(f'+f_c)\left(t_2-\frac{r_n}{c}\right)\right]\left(\frac{c}{f_c}\right)\phi_{\text{det}_n}\right\}$$
$$\times\exp\{-2r_n[\alpha(f+f_c)+\alpha(f'+f_c)]\}\exp\left[-j2\pi\left(\frac{2r_n}{c}\right)(f-f')\right]\left(\frac{1}{r_n^2}\right)\sin\theta_n, \tag{95}$$

where, from Eq. (48),

$$E\{F_n(f+f_c)F_n^*(f'+f_c)\} = D_T(k_1u_n,k_1v_n)D_T^*(k_2u_n,k_2v_n)E\{g_n(-\hat{n}_T,\hat{n}_T,f_1)g_n^*(-\hat{n}_T,\hat{n}_T,f_2)\}$$
$$\times D_R(k_1u_n,k_1v_n)D_R^*(k_2u_n,k_2v_n) \tag{96}$$

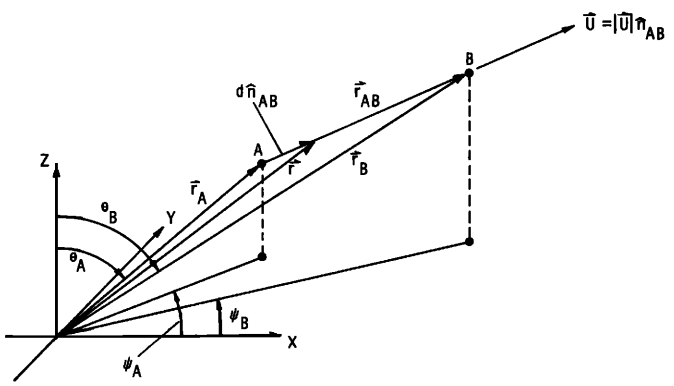

FIG. 5. Orientation of line target with respect to a monostatic transmit/receive array geometry.

and from Eq. (89),

$$\phi_{\mathrm{det}_n} = (2f_c/c)(|\mathbf{U}|/L)[u_n(|\mathbf{r}_B|u_B - |\mathbf{r}_A|u_A) + v_n(|\mathbf{r}_B|v_B - |\mathbf{r}_A|v_A) + w_n(|\mathbf{r}_B|w_B - |\mathbf{r}_A|w_A)], \tag{97}$$

where

$$u_n = \sin\theta_n \cos\psi_n, \quad v_n = \sin\theta_n \sin\psi_n, \tag{98}$$

and

$$w_n = \cos\theta_n$$

are the direction cosines of the nth highlight with respect to the positive x, y, and z axes, respectively.

The average monostatic (backscatter) radar cross section of the nth highlight is given by $4\pi E\{|g_n(-\hat{n}_T, \hat{n}_T, f_c)|^2\} \equiv 4\pi\sigma_{d_n}(-\hat{n}_T, \hat{n}_T, f_c)$, where $\sigma_{d_n}(-\hat{n}_T, \hat{n}_T, f_c)$ is the average differential backscattering cross section of the nth highlight. The *target strength* of the nth highlight is [see Eq. (70)]

$$10\log_{10}[\sigma_{d_n}(-\hat{n}_T, \hat{n}_T, f_c)/A_1]\,\mathrm{dB}\ re{:}\ A_1, \tag{99}$$

where $A_1 = 1\ \mathrm{m}^2$.

Since the target is being modeled as a linear array of N highlights (sources) reradiating in random phase (i.e., the N scattered fields are uncorrelated), the average differential backscattering cross section of the target is given by

$$\sigma_d(-\hat{n}_T, \hat{n}_T, f_c) \simeq \sum_{i=1}^{N} \sigma_{d_i}(-\hat{n}_T, \hat{n}_T, f_c) \tag{100}$$

since intensities add.[48] The corresponding *target strength* can be obtained by computing

$$10\log_{10}[\sigma_d(-\hat{n}_T, \hat{n}_T, f_c)/A_1]\,\mathrm{dB}\ re{:}\ A_1, \tag{101}$$

where $A_1 = 1\ \mathrm{m}^2$.

Both the coherence time and the coherence bandwidth, and hence, the frequency and time delay spreading associated with our target model, can be computed from Eq. (95). With the use of Eq. (95), the autocorrelation function $R_{\tilde{y}_{i'}}(t, t')$, which is given by Eq. (15) and appears in the SIR expression given by Eq. (14), can now be computed. Since Eq. (95) pertains to a monostatic geometry, the monostatic form of the volume reverberation two-frequency correlation

B. Scattering function

If it is assumed that the transmit signal is narrow band so that $|f|/f_c \ll 1$, $|f'|/f_c \ll 1$, and the approximate relationships given by Eqs. (54) through (56) are valid, then Eq. (95) reduces to

$$R_{H_T}(\Delta f, \Delta t) = \sum_{n=1}^{N} E\{|F_n(f_c)|^2\}\exp(-j2\pi\phi_{\mathrm{det}_n}\Delta t) \times \exp\{-j2\pi(r_n/c)[2 - (\phi_{\mathrm{det}_n}/f_c)]\Delta f\} \times \exp[-4\alpha(f_c)r_n](1/r_n^2)\sin\theta_n, \tag{102}$$

where $\Delta f = f - f'$, $\Delta t = t_1 - t_2$, and the third exponential involving attenuation in Eq. (95) was dropped [see Eq. (60)]. Now, upon substituting Eq. (102) into Eq. (22) and integrating, one obtains the following monostatic expression for the target scattering function:

$$R_{S_T}(\tau, \phi) = \sum_{n=1}^{N} \left(\frac{2 - (\phi_{\mathrm{det}_n}/f_c)}{c\tau_n}\right)^2 \times \exp(-4\alpha(f_c)\{(c\tau_n)/[2 - (\phi_{\mathrm{det}_n}/f_c)]\}) \times E\{|F_n(f_c)|^2\}\sin\theta_n\delta(\tau - \tau_n)\delta(\phi + \phi_{\mathrm{det}_n}), \tag{103}$$

where

$$\tau_n = (r_n/c)[2 - (\phi_{\mathrm{det}_n}/f_c)], \tag{104}$$

$$E\{|F_n(f_c)|^2\} = |D_T(ku_n, kv_n)|^2 E\{|g_n(-\hat{n}_T, \hat{n}_T, f_c)|^2\} \times |D_R(ku_n, kv_n)|^2, \tag{105}$$

and $k = 2\pi f_c/c$. Note that the time delay parameter τ_n given by Eq. (104) is *not* the round-trip time delay. However, as was discussed previously in Sec. IIB with regard to the volume reverberation scattering function, the round-trip delay can be computed from τ_n by dividing it by $[1 - (\phi_{\mathrm{det}_n}/f_c)]$, i.e., the round-trip time delay corresponding to the nth highlight is given by $\tau_n/[1 - (\phi_{\mathrm{det}_n}/f_c)]$. This will be demonstrated in Sec. IVB when a target scattering function is computed.

The scattering function given by Eq. (103) can be substituted into the SIR expression of Eq. (25). Since Eq. (103) pertains to a monostatic geometry, the monostatic form of the volume reverberation scattering function must therefore be used in Eq. (25) also.

IV. EXAMPLE PROBLEM CALCULATIONS

A. Volume reverberation scattering function

A computer solution of the volume reverberation scattering function will be presented for an example problem involving a monostatic transmit/receive array geometry.

The following monostatic form of the volume reverberation scattering function in spherical coordinates can be obtained from Eq. (64):

$$R_{S_R}(\tau, \phi) = \left(\frac{2 + (\phi/f_c)}{c\tau}\right)^2 \exp\left[-4\alpha(f_c)\left(\frac{c\tau}{2 + (\phi/f_c)}\right)\right] \times \int_{\theta=0}^{\pi/2}\int_{\psi=0}^{2\pi} \rho_V\left(\frac{c\tau}{2 + (\phi/f_c)}, \theta, \psi\right) \times E\{|F(f_c)|^2\}\, p_{\phi_{\mathrm{rnd}}}(\phi + \phi_{\mathrm{det}})\, d\psi \sin\theta\, d\theta; \tag{106}$$

$$\frac{R_U}{c}\left(2 + \frac{\phi}{f_c}\right) \geqslant \tau \geqslant \frac{R_L}{c}\left(2 + \frac{\phi}{f_c}\right),$$

where R_L and R_U are the lower and upper limits of integra-

tion with respect to range, respectively. It is assumed that the array lies in the XY plane. Thus the positive Z axis is normal to the face of the array. In this example problem, both the transmit and receive directivity functions are identical, i.e., $D_T = D_R = D$. As a result,

$$E\{|F(f_c)|^2\} = |D(ku, kv)|^4 E\{|g(-\hat{n}_T, \hat{n}_T, f_c)|^2\}, \tag{107}$$

where the directivity function actually used is

$$D(ku, kv) = \left[\sum_{n=1}^{5} Q_n \cos\left(\frac{(2n-1)\pi d}{\lambda}(u-u_0)\right) \Big/ \sum_{n=1}^{5} Q_n\right] \times \{\sin[(10\pi d/\lambda)v]/10\sin[(\pi d/\lambda)v]\}. \tag{108}$$

Equation (108) corresponds to a (10×10) planar array composed of 10-element, amplitude shaded, phase shifted, linear arrays parallel to the X axis and 10-element, uniformly shaded, linear arrays parallel to the Y axis where $Q_1 = 1.0$, $Q_2 = 0.8389$, $Q_3 = 0.5801$, $Q_4 = 0.3153$, $Q_5 = 0.1251$, and $d/\lambda = 0.4$. The parameter d is the uniform spacing (in meters) between elements and λ is the wavelength (in meters) corresponding to the frequency f_c (in hertz). The particular choice of amplitude shading coefficients ensures 40-dB down side-lobe levels in the XZ plane. The phase shift $u_0 = \sin\theta_0 \cos\psi_0$ is used for beam tilting in the XZ plane.

Assume that the array is in motion in the positive z direction and that the *relative*, deterministic velocity of the discrete point scatterers with respect to the array is $\mathbf{U} = -20.0\,\hat{z}$ m/s so that

$$\phi_{\text{det}} = -(40.0 f_c/c)\cos\theta \text{ Hz}. \tag{109}$$

Finally, for simplicity, also assume that the scatterers are uniformly distributed in space, i.e., $\rho_V = $ constant; and that the average differential backscattering cross section of an individual point scatterer is omnidirectional, i.e., $E\{|g(-\hat{n}_T, \hat{n}_T, f_c)|^2\}$ does not depend upon $\hat{n}_T$ and is, therefore, equal to a constant σ_d.

Let us first consider the case of relative, deterministic motion only. Using the aforementioned assumptions and replacing $p_{\phi_{\text{rnd}}}(\phi + \phi_{\text{det}})$ by $\delta(\phi + \phi_{\text{det}})$, Eq. (106) reduces to

$$R_{S_R}(\tau, \phi) = K \int_{\psi=0}^{2\pi} |D(ku, kv)|^4 d\psi \sin\theta, \tag{110}$$

where θ is such that

$$(40.0 f_c/c)\cos\theta = \phi \text{ Hz}; \quad \pi/2 \geqslant \theta \geqslant 0, \tag{111}$$

and

$$\frac{R_U}{c}\left(2 + \frac{\phi}{f_c}\right) \geqslant \tau \geqslant \frac{R_L}{c}\left(2 + \frac{\phi}{f_c}\right), \tag{112}$$

and where

$$K = \rho_V \left(\frac{2 + (\phi/f_c)}{c\tau}\right)^2 \exp\left[-4\alpha(f_c)\left(\frac{c\tau}{2 + (\phi/f_c)}\right)\right]\sigma_d. \tag{113}$$

Figures 6–8 are *normalized* Doppler profiles (range constant) of Eq. (110) for beam tilts of $\theta_0 = 0°$, $\psi_0 = 0°$; $\theta_0 = 30°$, $\psi_0 = 0°$; and $\theta_0 = 45°$, $\psi_0 = 0°$, respectively. The values of $c = 1500$ m/s, $\alpha(f_c) = 4.9\times 10^{-4}$ Np/m, and $f_c = 25$ kHz were used in connection with Figs. 6–8. Note the increase in Doppler spread, measured at the 3-dB down level, as the beam tilt angle θ_0 is increased. This is not surprising since as the beam tilt angle is increased, the beamwidth of the directivity pattern increases[49] which results in an increase in Doppler spread. Also observe from Fig. 6 that the scattering function peaks at $\phi = 664$ Hz, which corresponds to $\theta = 5°$, rather than peaking at $\phi = 667$ Hz, which corresponds to $\theta = \theta_0 = 0°$. This is due to the $\sin\theta$ dependence of the scattering function. At $\theta = 0°$, the elemental scattering volume dV is zero; and hence, there is no scattered power. Figures 6–8 correspond to relative deterministic motion only and demonstrate the effect of tilting a given beam pattern on frequency spread.

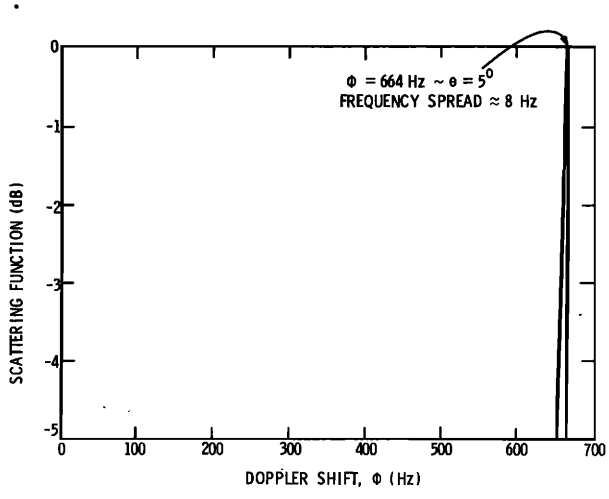

FIG. 6. Normalized Doppler profile of volume reverberation scattering function. Relative deterministic motion only ($\theta_0 = 0°$, $\psi_0 = 0°$).

If we now allow the discrete point scatterers to have random motion, Eq. (106) becomes

$$R_{S_R}(\tau, \phi) = K \int_{\psi=0}^{2\pi} \int_{\theta=0}^{\pi/2} |D(ku, kv)|^4 p_{\phi_{\text{rnd}}} \times [\phi - (40.0 f_c/c)\cos\theta]\sin\theta\, d\theta\, d\psi, \tag{114}$$

where it was assumed that the relative, deterministic velocity of the discrete point scatterers with respect to the array is $\mathbf{U} = -20.0\,\hat{z}$ m/s [see Eq. (109)], and where K is given by Eq. (113), the directivity function D by Eq. (108), and $p_{\phi_{\text{rnd}}}(\cdot)$

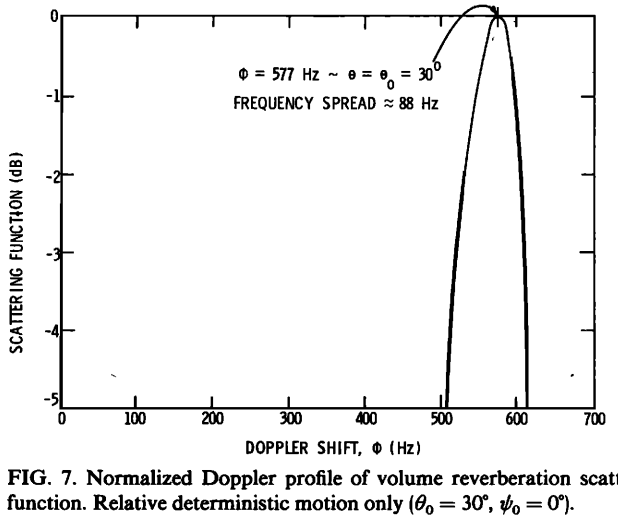

FIG. 7. Normalized Doppler profile of volume reverberation scattering function. Relative deterministic motion only ($\theta_0 = 30°$, $\psi_0 = 0°$).

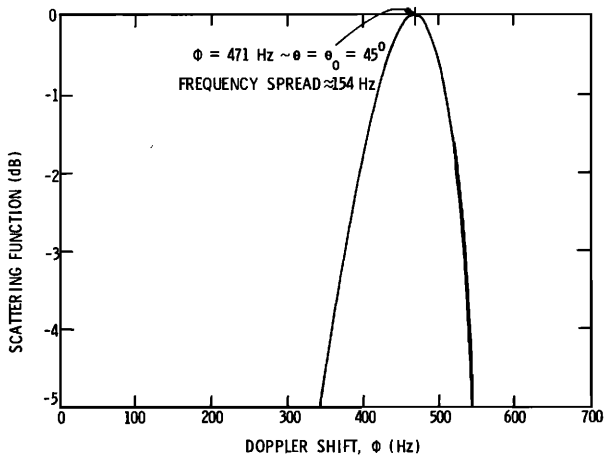

FIG. 8. Normalized Doppler profile of volume reverberation scattering function. Relative deterministic motion only ($\theta_0 = 45°$, $\psi_0 = 0°$).

by Eq. (68) with $\hat{n}_R = -\hat{n}_T$ and $\sigma = 1.0$ m/s (see Fig. 4). Figure 9 is a *normalized* Doppler profile of Eq. (114). The values of the parameters used for Fig. 9 are identical with those used for Fig. 8. By comparing Figs. 8 and 9, it is seen that an additional frequency spread of 26 Hz is introduced by the random motion of the scatterers for $\sigma = 1.0$ m/s. This represents an increase of approximately 17%.

B. Target scattering function

The target scattering function given by Eq. (103) is calculated for an example problem using the monostatic transmit/receive array geometry depicted in Fig. 10. In this example, the array is not in motion. The magnitude of the deterministic velocity of the target is $|\mathbf{U}| = 20.0$ m/s. The location of the endpoints A and B of the target with respect to the array when transmission at $t = 0$ begins is specified by the following constants: $|\mathbf{r}_A| = 500$ m, $\theta_A = \theta_B = 5.739°$, $\psi_A = 180°$, and $\psi_B = 0°$. The length of the target is $L = 100$ m. With this information, $|\mathbf{r}_B|$ can be calculated. The number of highlights being considered is $N = 10$. The first highlight is located 5 m from point A and the spacing between the remaining highlights thereafter is 10 m. The values $\theta_0 = 45°$, $\psi_0 = 0°$, $c = 1500.342$ m/s, $\alpha(f_c) = 4.9 \times 10^{-4}$ Np/m, and

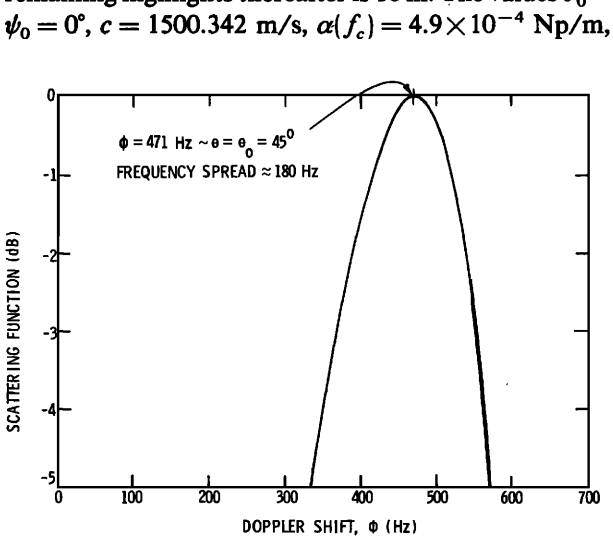

FIG. 9. Normalized Doppler profile of volume reverberation scattering function. Relative deterministic plus random motion ($\theta_0 = 45°$, $\psi_0 = 0°$).

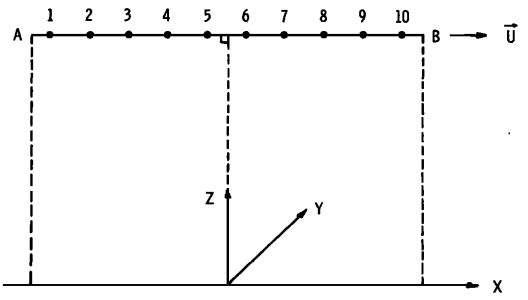

FIG. 10. Orientation of line target with respect to a monostatic transmit/receive array geometry for example target scattering function calculation.

$f_c = 25$ kHz are used. It is assumed that $D_T = D_R = D$, where the directivity function D is given by Eq. (108). It is also assumed that $E\{|g_n(-\hat{n}_T, \hat{n}_T, f_c)|^2\}$ is equal to a constant value σ_d which is the same for all N highlights.

Values for the *normalized* target scattering function, as a function of τ and ϕ, are presented in Table I. Upon inspecting Table I, it can be seen that highlights 1–5 have positive Doppler shifts which indicate that these five highlights are approaching the array which is in agreement with the geometry of the problem. Also note that highlights 6–10 have negative Doppler shifts which indicate that these five highlights are receding from the array which is also physically correct. Highlights 5 and 6 have Doppler shifts which are almost equal to zero since the position vectors $\mathbf{r}_5$ and $\mathbf{r}_6$ for these two highlights are nearly perpendicular to the line target. Note that the magnitude of the scattering function is larger for highlights 6–10 as compared to highlights 1–5. And, in fact, the scattering function has its maximum value at highlight 8. This is also in agreement with the geometry of the problem since the beam pattern was tilted in the general direction of highlights 6–10.

Note that the values for τ_n appearing in Table I do not correspond to round-trip time delays.

Table II presents values for the range r_n, the simple round-trip time delay $2r_n/c$, and the actual round-trip time delay $\tau_n/[1 - (\phi_{\text{det}_n}/f_c)]$, for the ten highlights. The simple round-trip time delay does not depend upon Doppler shift while the actual round-trip time delay does. The range values r_n (at $t = 0$ when transmission begins) were computed from Eq. (91). Upon inspecting Table II, it can be seen that the actual round-trip time delays for highlights 1–5 are *smaller* than the corresponding simple round-trip time de-

TABLE I. Normalized target scattering function.

Highlight n	$\tau = \tau_n$ (s)	$\phi = -\phi_{\text{det}_n}$ (Hz)	$R_{S_T}(\tau,\phi)$ (dB)
1	0.666 680	59.851	−0.376 507E 02
2	0.665 438	46.579	−0.243 289E 02
3	0.664 461	33.255	−0.107 524E 02
4	0.663 752	19.888	−0.592 028E 01
5	0.663 310	6.481	−0.686 279E 01
6	0.663 137	−6.858	−0.511 047E 01
7	0.663 231	−20.276	−0.328 704E 00
8	0.663 592	−33.638	−0.000 000E 00
9	0.664 220	−46.960	−0.294 615E 01
10	0.665 115	−60.229	−0.109 380E 02

TABLE II. Round-trip time delay calculations.

Highlight n	r_n (m)	$2r_n/c$ (s)	$\tau_n/[1-(\phi_{\text{det}_n}/f_c)]$ (s)
1	499.526	0.665 882 8	0.665 087 7
2	498.728	0.664 819	0.664 200 5
3	498.128	0.664 019 2	0.663 578 3
4	497.730	0.663 488 7	0.663 224 4
5	497.531	0.663 223 4	0.663 138 1
6	497.534	0.663 227 4	0.663 318 9
7	497.738	0.663 499 3	0.663 769 3
8	498.143	0.664 039 2	0.664 486
9	498.747	0.664 844 4	0.665 47
10	499.552	0.665 917 5	0.666 721 1

lays since these five highlights have positive Doppler shifts and are therefore approaching the array. Similarly, the actual round-trip time delays for highlights 6–10 are *larger* than the corresponding simple round-trip time delays since these five highlights have negative Doppler shifts and are therefore receding from the array.

V. SUMMARY

This paper considered the problem of detecting a doubly spread target return in the presence of reverberation and noise. Both the target and reverberation returns were modeled as the outputs from linear, time-varying, random filters.

Signal-to-interference ratio (SIR) expressions for a doubly spread target were derived for both broadband and narrow-band transmit signals. It was shown that in the broadband case, the SIR is dependent upon target and reverberation two-frequency correlation functions and upon the transmit and processing waveforms. For WSSUS communication channels, the narrow-band case, the SIR is dependent upon the target and reverberation scattering functions and the cross-ambiguity function of the transmit and processing waveforms. The term "narrow band" was used to describe a transmit signal vis-à-vis "broadband" whenever the values of the frequency dependent functions such as directivity patterns, differential scattering cross sections, and attenuation coefficients due to sound absorption could be approximated by their values at the center or carrier frequency.

Both volume reverberation and target two-frequency correlation functions and scattering functions were *derived*. In the past, *assumed* functional forms for the reverberation (clutter) scattering function were used in order to calculate the SIR.

Volume reverberation was modeled as the spatially uncorrelated scattered acoustic pressure field from randomly distributed discrete point scatterers in deterministic plus random translational motion. The point scatterers were distributed in space according to an aribtrary volume density function with dimensions of number of scatterers per unit volume.

The two-frequency correlation function representing the volume reverberation communication channel was derived for a bistatic transmit/receive planar array geometry. A single scattering approximation was used and frequency dependent attenuation of sound pressure amplitude due to absorption was included. General, frequency dependent transmit and receive directivity patterns were also included. The scattered fields from different regions within the scattering volume were assumed to be uncorrelated.

Using a narrow-band assumption, a bistatic expression for the volume reverberation scattering function was obtained from the two-frequency correlation function via a two-dimensional Fourier transformation. It was shown to include explicitly all the important system functions and physical parameters as opposed to having them lumped together and accounted for by a single random variable as has been done in the past. A probability density function of random Doppler shift due to the random motion of the scatterers was also derived. Computer plots of the density function were presented for a monostatic geometry as a function of the standard deviation of the random motion of the scatterers. In addition, the average received energy from volume reverberation was computed from the monostatic form of the volume reverberation scattering function. Using several simplifying assumptions, it was shown to reduce to the sonar equation for the reverberation level.

The doubly spread target was modeled as a linear array of discrete highlights in deterministic translational motion with respect to a monostatic transmit/receive array geometry. The target two-frequency correlation function was obtained from the monostatic form of the volume reverberation two-frequency correlation function by appropriately specifying the volume density function of the highlights.

Using a narrow-band assumption, a monostatic expression for the target scattering function was obtained from the two-frequency correlation function via a two-dimensional Fourier transformation.

Computer simulation results for both the volume reverberation and target scattering functions were presented for example problems involving a monostatic transmit/receive array geometry. The volume reverberation scattering function predicted frequency spreading as a function of both beam tilt angle and random motion of the discrete point scatterers. As one might expect, frequency spread increased as both beam tilt angle and random motion increased. Also predicted was time spread and/or contraction as a function of Doppler shift. Similarly, the target scattering function predicted a spread in Doppler values and a time spread and/or contraction as a function of Doppler shift.

ACKNOWLEDGMENT

The work described in this paper was supported by NAVSEA Undersea Weapons Guidance and Control Block, Code NSEA 63R-14.

APPENDIX

Consider the random variable [Eq. (69)]

$$\phi_{\text{rnd}} \triangleq f_c(\hat{n}_T - \hat{n}_R)\cdot\mathbf{V}_f/c = f_c|\hat{n}_T - \hat{n}_R|\,|\mathbf{V}_f|\cos\xi/c,$$

where it is assumed that $|\mathbf{V}_f|$ is Maxwell distributed, the angle ξ is uniformly distributed, and that the random variables $|\mathbf{V}_f|$ and $\cos\xi$ are statistically independent. In order for $|\mathbf{V}_f| = (V_{f_x}^2 + V_{f_y}^2 + V_{f_z}^2)^{1/2}$ to be Maxwell distributed, the

three components V_{f_x}, V_{f_y}, and V_{f_z} must be statistically independent Gaussian random variables, each with zero mean and variance σ^2 (e.g., see Papoulis[50]).

In order to derive the probability density function of $\phi_{\rm rnd}$, first rewrite Eq. (69) as

$$\phi_{\rm rnd} = XY, \tag{A1}$$

where

$$X = a|\mathbf{V}_f|, \tag{A2}$$

$$Y = \cos\xi, \tag{A3}$$

and

$$a = f_c|\hat{n}_T - \hat{n}_R|/c. \tag{A4}$$

Note that $E\{\phi_{\rm rnd}\} = E\{X\}E\{Y\} = 0$ since $E\{\cos\xi\} = 0$ when ξ is uniformly distributed.[51] Since X and Y are statistically independent random variables, the probability density function of $\phi_{\rm rnd}$ is given by[52]

$$p_{\phi_{\rm rnd}}(\phi) = \int_{-\infty}^{\infty} \frac{1}{|x|} p_X(x) p_Y\left(\frac{\phi}{x}\right) dx, \tag{A5}$$

where[50,53]

$$p_X(x) = (1/|a|)\, p_{|\mathbf{V}_f|}(x/a), \tag{A6}$$

$$p_{|\mathbf{V}_f|}\left(\frac{x}{a}\right) = \begin{cases} \left(\frac{2}{\pi}\right)^{1/2}\left(\frac{1}{\sigma^3}\right)\left(\frac{x}{a}\right)^2 \exp\left[-\left(\frac{1}{2}\right)\left(\frac{x}{a\sigma}\right)^2\right]; & x \geqslant 0, \\ 0; & x < 0, \end{cases} \tag{A7}$$

and[51,54]

$$p_Y\left(\frac{\phi}{x}\right) = \begin{cases} 1/\{\pi[1-(\phi/x)^2]^{1/2}\}; & |\phi/x| < 1, \\ 0; & |\phi/x| > 1. \end{cases} \tag{A8}$$

Note that the probability that $(\phi/x) = \pm 1$ is zero.[54] Substituting Eqs. (A6)–(A8) into Eq. (A5) yields

$$p_{\phi_{\rm rnd}}(\phi) = \left(\frac{c}{|\hat{n}_T - \hat{n}_R|\, f_c\sigma}\right)^3 \frac{\sqrt{2}}{\pi\sqrt{\pi}} \times \int_{-\infty}^{\infty} \frac{1}{|x|} \frac{1}{[1-(\phi/x)^2]^{1/2}} x^2 \times \exp\{-(\tfrac{1}{2})[c/(|\hat{n}_T - \hat{n}_R|\, f_c\sigma)]^2 x^2\} dx;$$

$$x \geqslant 0, \quad |\phi/x| < 1, \tag{A9}$$

or

$$p_{\phi_{\rm rnd}}(\phi) = \left(\frac{c}{|\hat{n}_T - \hat{n}_R|\, f_c\sigma}\right)^3 \frac{\sqrt{2}}{\pi\sqrt{\pi}} \int_{|\phi|}^{\infty} \frac{x^2}{(x^2-\phi^2)^{1/2}} \times \exp\{-(\tfrac{1}{2})[c/(|\hat{n}_T - \hat{n}_R|\, f_c\sigma)]^2 x^2\} dx;$$

$$|\phi| < x < \infty, \tag{A10}$$

which is the probability density function of the random Doppler shift $\phi_{\rm rnd}$.

[1] A. Ishimaru, *Wave Propagation and Scattering in Random Media* (Academic, New York, 1978), Vol. I, Chap. 5, p. 95.

[2] H. L. Van Trees, *Detection, Estimation and Modulation Theory* (Wiley, New York, 1971), Vol. III, pp. 572–574.

[3] A. D. Whalen, *Detection of Signals in Noise* (Academic, New York, 1971), Chap. 3, pp. 73, 74.

[4] A. W. Ellinthorpe and A. H. Nuttall, "Theoretical and Empirical Results on the Characterization of Undersea Acoustic Channels," in *IEEE First Annual Communication Convention* (1965), pp. 585–591.

[5] D. Middleton, "A Statistical Theory of Reverberation and Similar First-Order Scattered Fields. Part I: Waveforms and the General Process," IEEE Trans. Inform. Theory **13**, 372–392 (1967).

[6] K. A. Sostrand, "Mathematics of the Time-Varying Channel," in *Proceedings of NATO Advanced Study Institute on Signal Processing with Emphasis on Underwater Acoustics* (Enschede, The Netherlands, 1968), Vol. II, pp. (25-1)–(25-20).

[7] See Ref. 2, Vol. III, Chap. 13, pp. 459–460.

[8] J. Johnsen, "Spectrum Analysis of Reverberation," in *Signal Processing*, edited by J. W. R. Griffiths, P. L. Stocklin, and C. Van Schooneveld (Academic, New York, 1973), pp. 97–115.

[9] R. Laval, "Sound Propagation Effects on Signal Processing," in *Signal Processing*, edited by J. W. R. Griffiths, P. L. Stocklin, and C. Van Schooneveld (Academic, New York, 1973), pp. 223–241.

[10] P. H. Moose, "Signal Processing in Reverberant Environments," in *Signal Processing*, edited by J. W. R. Griffiths, P. L. Stocklin, and C. Van Schooneveld (Academic, New York, 1973), pp. 413–428.

[11] R. Laval, "Time-Frequency-Space Generalized Coherence and Scattering Functions," in *Aspects of Signal Processing*, edited by G. Tacconi (Reidel, Dordrecht, The Netherlands, 1977), Vol. I, pp. 69–87.

[12] See Ref. 1, pp. 93–94.

[13] A. B. Baggeroer, "Sonar Signal Processing," in *Applications of Digital Signal Processing*, edited by A. V. Oppenheim (Prentice-Hall, Englewood Cliffs, NJ, 1978), Chap. 6, pp. 365, 366.

[14] P. E. Green, Jr., "Radar Measurements of Target Scattering Properties," in *Radar Astronomy*, edited by J. V. Evans and T. Hagfors (McGraw-Hill, New York, 1968), Chap. 1, pp. 1–77.

[15] P. A. Bello, "Characterization of Randomly Time-Variant Linear Channels," IEEE Trans. Commun. Syst. **11**, 360–393 (1963).

[16] R. S. Kennedy, *Fading Dispersive Communication Channels* (Wiley–Interscience, New York, 1969).

[17] W. D. Rummler, "Clutter Suppression by Complex Weighting of Coherent Pulse Trains," IEEE Trans. Aerospace Electron. Syst. **2**, 689–699 (1966).

[18] D. F. DeLong, Jr., and E. M. Hofstetter, "On the Design of Optimum Radar Waveforms for Clutter Rejection," IEEE Trans. Inform. Theory **13**, 454–463 (1967).

[19] W. D. Rummler, "A Technique for Improving the Clutter Performance of Coherent Pulse Train Signals," IEEE Trans. Aerospace Electron. Syst. **3**, 898–906 (1967).

[20] J. S. Thompson and E. L. Titlebaum, "The Design of Optimal Radar Waveforms for Clutter Rejection Using the Maximum Principle," Suppl. IEEE Trans. Aerospace Electron. Syst. **3** (6), 581–589 (1967).

[21] L. J. Spafford, "Optimum Radar Signal Processing in Clutter," IEEE Trans. Inform. Theory **14**, 734–743 (1968).

[22] C. A. Stutt and L. J. Spafford, "A Best Mismatched Filter Response for Radar Clutter Discrimination," IEEE Trans. Inform. Theory **14**, 280–287 (1968).

[23] D. F. DeLong, Jr., and E. M. Hofstetter, "The Design of Clutter-Resistant Radar Waveforms with Limited Dynamic Range," IEEE Trans. Inform. Theory **15**, 376–385 (1969).

[24] L. H. Sibul and E. L. Titlebaum, "Signal Design for Detection of Targets in Clutter," Proc. IEEE **69**, 481–482 (1981).

[25] T. Kooij, "Optimum Signals in Noise and Reverberation," in *Proceedings of NATO Advanced Study Institute on Signal Processing with Emphasis on Underwater Acoustics* (Enschede, The Netherlands, 1968), Vol. I, pp. (17-1)–(17-12).

[26] See Ref. 2.

[27] D. Middleton, "A Statistical Theory of Reverberation and Similar First-Order Scattered Fields. Part II: Moments, Spectra, and Special Distributions," IEEE Trans. Inform. Theory **13**, 393–414 (1967).

[28] J. F. McDonald and F. B. Tuteur, "Calculation of the Range-Doppler Plot for a Doubly Spread Surface-Scatter Channel atHigh Rayleigh Parameters," J. Acoust. Soc. Am. **57**, 1025–1029 (1975).

[29] F. B. Tuteur, J. F. McDonald, and H. Tung, "Second-Order Statistical Moments of a Surface Scatter Channel with Multiple Wave Direction and Dispersion," IEEE Trans. Commun. **24**, 820–831 (1976).

[30] L. J. Ziomek, "Generalized Kirchhoff Approach to the Ocean Surface-Scatter Communication Channel. Part II: Second Order Functions," J. Acoust. Soc. Am. **71**, 1487–1495 (1982).

[31] See Ref. 1, pp. 96–98.

[32]See Ref. 1, p. 100.
[33]L. J. Ziomek, "A Scattering Function Approach to Underwater Acoustic Detection and Signal Design," Ph.D. dissertation, The Pennsylvania State University (1981), Chap. 3, pp. 66–74.
[34]See Ref. 33, Chap. 6, pp. 191–240.
[35]P. Faure, "Theoretical Model of Reverberation Noise," J. Acoust. Soc. Am. **36**, 259–266 (1964).
[36]R. J. Urick, *Principles of Underwater Sound* (McGraw–Hill, New York, 1975), 2nd ed., Chap. 8, pp. 211, 212.
[37]C. S. Clay and H. Medwin, *Acoustical Oceanography: Principles and Applications* (Wiley–Interscience, New York, 1977), Chaps. 6 and 7.
[38]See Ref. 1, Chap. 4, pp. 69–73.
[39]P. M. Morse and K. U. Ingard, *Theoretical Acoustics* (McGraw–Hill, New York, 1968), Chap. 7, p. 377.
[40]See Ref. 1, Chap. 2, pp. 10, 39, and 40.
[41]See Ref. 33, Appendix A, pp. 260–266.
[42]L. J. Ziomek, "Comments on the Generalized Ambiguity Function," IEEE Trans. Acoust. Speech, Signal Process. **ASSP-30**, 117–119 (1982).
[43]D. Middleton, "Doppler Effects for Randomly Moving Scatterers and Platforms," J. Acoust. Soc. Am. **61**, 1231–1250 (1977).
[44]See Ref. 36, pp. 212–218.
[45]See Ref. 37, Chap. 6, pp. 181–182, and Chap. 7, p. 234.
[46]See Ref. 33, Chap. 2, pp. 42, 43.
[47]V. V. Ol'shevskii, *Characteristics of Sea Reverberation* (Consultants Bureau, New York, 1967).
[48]See Ref. 37, Chap. 7, p. 220.
[49]B. D. Steinberg, *Principles of Aperture and Array System Design* (Wiley–Interscience, New York, 1976), Chap. 3, pp. 47–49.
[50]A. Papoulis, *Probability, Random Variables, and Stochastic Processes* (McGraw–Hill, New York, 1965), Chap. 8, p. 273.
[51]R. E. Ziemer and W. H. Tranter, *Principles of Communications* (Houghton Mifflin, Boston, 1976), Chap. 4, p. 189.
[52]W. B. Davenport, Jr., *Probability and Random Processes* (McGraw–Hill, New York, 1970), Chap. 6, p. 207.
[53]See Ref. 50, Chap. 5, p. 127.
[54]See Ref. 50, Chap. 5, pp. 132–134.

Broadband and narrow-band signal-to-interference ratio expressions for a doubly spread target

Lawrence J. Ziomek, and Leon H. Sibul

Citation: The Journal of the Acoustical Society of America **72**, 804 (1982); doi: 10.1121/1.388260
View online: https://doi.org/10.1121/1.388260
View Table of Contents: http://asa.scitation.org/toc/jas/72/3
Published by the Acoustical Society of America